

Tetra- versus Pentavalent Inhibitors of Cholera Toxin**

Ou Fu,^[a] Aliaksei V. Pukin,^[a] H. C. Quarles van Ufford,^[a] Thomas R. Branson,^[a, b] Dominique M. E. Thies-Weesie,^[c] W. Bruce Turnbull,^[b] Gerben M. Visser,^[d] and Roland J. Pieters^{*[a]}

The five B-subunits (CTB₅) of the *Vibrio cholerae* (cholera) toxin can bind to the intestinal cell surface so the entire AB₅ toxin can enter the cell. Simultaneous binding can occur on more than one of the monosialotetrahexosylganglioside (GM1) units present on the cell surface. Such simultaneous binding arising from the toxin's multivalency is believed to enhance its affinity. Thus, blocking the initial attachment of the toxin to the cell surface using inhibitors with GM1 subunits has the potential to stop the disease. Previously we showed that tetravalent GM1 molecules were sub-nanomolar inhibitors of CTB₅. In this study,

we synthesized a pentavalent version and compared the binding and potency of penta- and tetravalent cholera toxin inhibitors, based on the same scaffold, for the first time. The pentavalent geometry did not yield major benefits over the tetravalent species, but it was still a strong inhibitor, and no major steric clashes occurred when binding the toxin. Thus, systems which can adopt more geometries, such as those described here, can be equally potent, and this may possibly be due to their ability to form higher-order structures or simply due to more statistical options for binding.

Introduction

The cholera disease is a major source of suffering around the world. This diarrheal disease is caused by the *Vibrio cholerae* bacteria, but it is the cholera toxin (CT) it produces that is the actual pathogenic species. The toxin attaches itself to the intestinal cell wall where it is subsequently internalized and the A-subunit of this AB₅ toxin^[1] subsequently initiates the disease by raising the cellular cyclic adenosine monophosphate (cAMP) concentration followed by fluid efflux into the intestines.^[2] The initial attachment of the toxin to the intestinal cell surface is caused by the five B-subunits (CTB₅) that surround the A-subunit. While a single B binding site already binds with nanomolar

affinities to a GM1-oligosaccharide (GM1os), simultaneous binding of more than one B-subunit of the toxin can greatly enhance its affinity (Figure 1). Blocking the initial attachment of the toxin to the cell surface has the potential to block the disease. Considering the fact that the toxin itself takes advantage of multivalency^[3,4] in its binding to the cell surface, it was clear that, in order to interfere effectively, a multivalent ligand system would have to be designed.

Several evaluated multivalent systems have been designed based on dendrimers,^[5,6] polymers^[7,8] peptides,^[9] and also pentavalent scaffolds^[10–12] and have clearly shown the promise of the multivalency approach.^[13–16] In one such approach we attached the GM1os to dendritic scaffolds of varying valencies. Especially effective were the tetra- and octavalent systems, which were able to inhibit CTB₅ at subnanomolar concentrations and with potency enhancements orders of magnitude larger than the corresponding monovalent ligand.^[17]

Subsequent studies with the close relative of the cholera toxin, the heat labile enterotoxin of *E. coli* (LT), showed that the multivalent ligands, when mixed with the toxin, would lead to aggregates involving many toxin molecules.^[18] This was shown by analytical ultracentrifuge experiments as well as by atomic force microscopy. The observed aggregation was attributed to the mismatch in valency between the multivalent ligand (four or eight) and the multisubunit toxin (five). In fact, it was considered a possibility that the enormous potency enhancements observed in the inhibition assay with the cholera toxin could be due to the mismatch and the subsequent aggregation that the multivalent ligands initiated. On the other hand, there were reports in the literature, which described symmetrical pentavalent CT or LT ligands that were shown to be potent toxin inhibitors that clearly formed a 1:1 complex with the toxin, as judged by dynamic light scattering (DLS) ex-

[a] O. Fu, Dr. A. V. Pukin, H. C. Q. van Ufford, Dr. T. R. Branson, Prof. Dr. R. J. Pieters
Department of Medicinal Chemistry and Chemical Biology
Utrecht University, P.O. Box 80082, 3508 TB Utrecht (The Netherlands)
E-mail: R.J.Pieters@uu.nl

[b] Dr. T. R. Branson, Dr. W. B. Turnbull
School of Chemistry and Astbury Centre for Structural Molecular Biology
University of Leeds, Leeds LS2 9JT (United Kingdom)

[c] Dr. D. M. E. Thies-Weesie
Van 't Hoff Laboratory for Physical and Colloid Chemistry
Debye Institute for Nanomaterials Science, Utrecht University
Padualaan 8, 3584 CH Utrecht (The Netherlands)

[d] Dr. G. M. Visser
Department of Infectious Diseases and Immunology
Faculty of Veterinary Medicine, Utrecht University
PO Box 80.165, 3508 TD Utrecht (The Netherlands)

[**] This article is part of the Virtual Issue "Carbohydrates in the 21st Century: Synthesis and Applications".

Supporting information for this article is available on the WWW under <http://dx.doi.org/10.1002/open.201500006>.

© 2015 The Authors. Published by Wiley-VCH Verlag GmbH & Co. KGaA. This is an open access article under the terms of the Creative Commons Attribution-NonCommercial License, which permits use, distribution and reproduction in any medium, provided the original work is properly cited and is not used for commercial purposes.

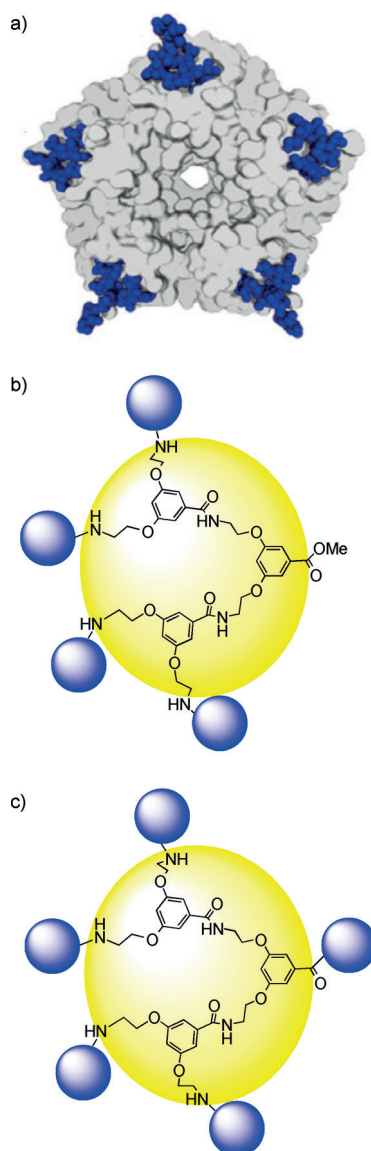


Figure 1. a) X-ray structure of the cholera toxin B-subunit (CTB) bound to GM1os (PDB ID: 3CHB); b, c) General architecture of the tetravalent (b) and pentavalent (c) ligands described here.

periments.^[10] Based on the 1:1 design, several pentavalent CT inhibitors were reported, and it was suggested that this design was beneficial to the inhibition.^[11,12] This also included a modified version of the cholera toxin that can no longer bind GM1 and was outfitted with 5 GM1os ligands.^[19] The related Shiga-like toxin has also seen a potent inhibitor with five arms for each subunit.^[20] Potent inhibition was seen, although the binding mode, involving two toxins, was not as expected, as the two ligands per arm engaged two separate toxins rather than two binding sites per toxin subunit. However, so far, no experiments were undertaken that compared a matching pentavalent CT inhibitor with inhibitors of nonmatching valencies based on closely related scaffolds. Therefore, it remains very much unclear which of the two approaches—1:1 design or mismatch-aggregation—is the best. We now address this question and report on the synthesis and evaluation in the same

assay of tetra- and pentavalent GM1-based ligand systems for CT inhibition.

Results and Discussion

Synthesis

The synthesis started with the preparation of the scaffold for the tetravalent inhibitor **5**, which was subsequently used for the preparation of the scaffold for the pentavalent inhibitor **8** (Scheme 1). The overall design of the tetravalent inhibitor was kept close to the previous version (inhibitor **11**)^[17] although there were differences in the spacer arms due to the availability and use of a different GM1os building block, that is, **6** in this case. The length of the spacer arm was almost the same as before, with the present one just measuring two atoms longer. Furthermore, the previous partly hydrophobic and partly hydrophilic spacer arm was now replaced by one consisting almost entirely of hydrophilic ethylene glycol units.

The synthesis started with the elongation of the four arms of **1** as previously described.^[5] The spacer **2**^[21] was coupled to the dendritic scaffold **1** by the action of benzotriazol-1-yloxytris(dimethylamino)-phosphonium hexafluorophosphate (BOP) and *N,N*-diisopropylethylamine (DIPEA), which resulted in **3** in 50% yield. After that, trifluoroacetic acid (TFA) was used to remove the Boc protecting group from the amino groups of **3**, and a coupling reaction between **3** and **4**^[22] using 1-[bis(dimethylamino)methylene]-1H-1,2,3-triazolo[4,5-b]pyridinium 3-oxid hexafluorophosphate (HATU) and DIPEA afforded the tetrameric full length scaffold **5** in 60% yield over two steps. Microwave-assisted copper(I)-catalyzed azide-alkyne cycloaddition (CuAAC) was subsequently used to conjugate the GM1os derivative **6** to the scaffold **5**, which efficiently yielded the tetravalent GM1 derivative **7**. The latter was purified by preparative high-performance liquid chromatography (HPLC).

The tetravalent scaffold **5** formed the starting point for the synthesis of the pentavalent version (Scheme 1, steps e–g). To this end, the methyl ester of **5** was saponified quantitatively by base. The resulting carboxylic acid was coupled to the commercially available spacer **9** using BOP and DIPEA, which successfully gave **8** as the pentavalent scaffold in 51% yield over two steps. Subsequently, a microwave-assisted CuAAC conjugation reaction was employed on **8** and **6** leading to the formation of the pentavalent GM1 derivative **10**, which was purified by preparative HPLC.

Inhibition

The compounds were evaluated as CTB₅ inhibitors using an assay similar to an enzyme-linked immunosorbent assay (ELISA), as previously described.^[17] A 96-well ELISA plate was coated by the natural bovine brain GM1 ganglioside. The remaining binding sites were blocked with bovine serum albumin (BSA). Horseradish peroxidase (HRP)-conjugated CTB₅ was incubated with varying concentrations of the tested inhibitors for 2 h at room temperature. After that, the remaining activity of CTB₅ was measured upon addition of the solutions to the

wells and incubation for 30 min at room temperature to allow for binding of the remaining toxin. After incubation and washing, the amount of bound toxin was quantified by using a chromogenic substrate for HRP. The previously reported^[17] tetravalent GM1 compound **11** was used here as a reference in inhibitory potency evaluation. In the present assay, **11** showed an IC_{50} of 190 μM , a value close to the previously reported one (230 μM) (Table 1). The new tetravalent GM1 compound **7** ex-

Compound	Valency	IC_{50} [nM]
11	4	0.19 (± 0.02)
7	4	0.16 (± 0.04)
10	5	0.26 (± 0.02)

[a] Determined in an ELISA-like assay with CTB₅-HRP (40 ng/mL) and wells coated with GM1.

hibited a very similar inhibitory potency, with an IC_{50} of 160 μM . This result shows that a slightly different spacer length and considerably different spacer polarity did not lead to significantly different inhibitory properties. The pentavalent GM1 derivative **10** exhibited an IC_{50} of 260 μM , which is in the same range as the values found for both of the tetravalent ligands. This indicates that in our assay, the potency of the ligand of matching valency does not essentially differ from the potencies of its nonmatching analogues.

Sedimentation velocity analytical ultracentrifugation (SV-AUC)

In order to learn whether the pentavalent geometry of **10** leads to a different, possibly less aggregative, binding mode, SV-AUC^[23,24] experiments were undertaken. First a sample with just CTB₅ was measured. It contained a single species with a sedimentation coefficient of 4.4 S corresponding to a mass of 58 kDa for the protein pentamer. Sisu et al.^[18] previously used SV-AUC to test the tetrameric GM1os dendrimer **11** with LTB₅, and it was found to strongly aggregate the protein while no discrete oligomers were observed. In the present experiments, tetravalent inhibitor **7**, which is structurally similar to **11**, was added to CTB₅ at a pentamer concentration of 50 μM . With the addition of 0.2–1.0 equivalents, a dramatic reduction in the overall signal was observed, as had previously been shown for **11** and LTB₅, indicating rapid sedimentation of aggregating large particles (Figure 2, see also Supporting Information). However, with inhibitor **7**, the emergence of a peak at 7.2 ± 0.2 S was seen with a predicted mass of approximately 110 kDa, which corresponds to a dimer of CTB pentamers. With increasing amounts of inhibitor up to 10 equivalents, the amount of the dimer species increased, and the emergence of some stable CTB pentamers was also observed. Excess and unbound inhibitor was observed as a peak at 0.9 ± 0.1 S corresponding to a mass of 8 kDa.

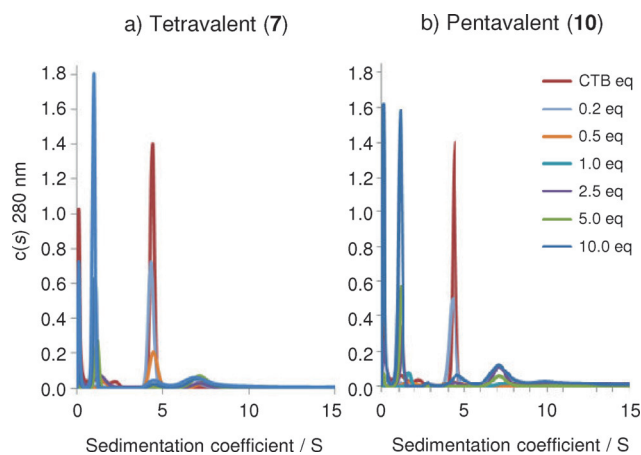


Figure 2. Sedimentation velocity analytical ultracentrifugation profiles of tetravalent **7** (a) and pentavalent **10** (b), recorded with increasing amounts of multivalent ligand (legend for both graphs).

Pentavalent inhibitor **10** matched the number of ligand groups to the number of binding sites of CTB₅ and so it was expected that this inhibitor should form stable 1:1 complexes. However, the AUC results were very similar to those observed for tetravalent ligand **7**. A reduction in signal indicated large scale aggregation, and some dimerization of CTB pentamers was observed. Again, at higher equivalents of inhibitor, some CTB pentamers were seen but with no significant difference to the tetravalent inhibitor.

Conclusions

For the first time, penta- and tetravalent cholera toxin inhibitors based on the same scaffold were compared. The structures contained arms of sufficient length to simultaneously bridge all binding sites (see Supporting Information). Clearly, the pentavalent geometry of **10** did not yield major benefits over the tetravalent **7**; in fact, it was a little worse. However, it was still a strong inhibitor, so major steric clashes did not occur in the binding of **10** to the toxin. Nevertheless one can argue that the potency per arm is significantly reduced by a factor of about two. Both **7** and **10** behaved very similarly in sedimentation velocity analytical ultracentrifugation (SV-AUC). As noted before for **11**, aggregation occurs upon toxin binding, resulting in higher order structures, while only minor amounts of bound pentamer (or its dimer) could be detected. The arms of the systems described here are designed in agreement with the concept that their 'effective length'^[10] should match the distance they should cover. The lengths of their extended conformations are therefore far longer. While the fifth arm is slightly shorter than the other four, it should be kept in mind that it is easily capable of bridging the fifth site, and that is attached to a different site of the scaffold.

It is of interest to compare our results to related pentavalent systems in the literature. Even though inhibition assay results cannot be directly compared, it is a fact that the same assay is used in these studies. One pentavalent GM1 system, based on a corranulene scaffold, exhibited an IC_{50} of 5 nM, presumably

not living up to its full potential due to self-association of the scaffold.^[12] A related calix[5]arene-based system showed higher potency with an IC_{50} of 450 μM .^[11] Neither of these systems showed a compelling argument in favor of a pentavalent system, consistent with our results. CTB_5 , whose binding sites were disabled, was recently used as a scaffold for the display of five GM1 units. This construct showed an IC_{50} of 104 μM and was shown to form a 1:1 complex with the toxin. While impressive, it is not very different from the 160 μM observed here, nor the 50 μM value for our previously reported octavalent GM1 structure.^[17]

It seems that a preorganized system can indeed bind in a 1:1 fashion with CTB_5 ,^[19] however, systems which can adopt more geometries, such as those described here, can be equally potent, and this may possibly be due to their ability to form higher-order structures or simply due to more statistical options for binding. Bundle and Kitov provided theoretical support for the latter to explain the enhancements in the inhibition of AB_5 toxins.^[25] Their model emphasized the importance of a statistical term that describes in how many ways a multivalent ligand can bind to multiple binding sites—this was called avidity entropy. This was used to explain why an octavalent system was a better Shiga-like toxin inhibitor than the matched pentavalent one.

Experimental Section

General remarks: Unless stated otherwise, chemicals were obtained from commercial sources and used without further purification. Solvents were purchased from Biosolve (Valkenswaard, the Netherlands). Acid spacers **2**^[13] and **4**^[22] were synthesized following literature procedures. Compound **6** was purchased from Elicityl (Crolles, France). Microwave reactions were carried out in a dedicated microwave oven: the Biotage Initiator (Uppsala, Sweden). The microwave power was limited by temperature control once the desired temperature was reached. A sealed vessel of 2–5 mL was used. Analytical HPLC runs were performed on a Shimadzu automated HPLC system (Kyoto, Japan) with a reversed-phase column (ReproSpher 100, C8, 5 μm , 250X4.6 mm, Dr. Maisch GmbH, Ammerbuch-Entringen, Germany), equipped with an evaporative light-scattering detector, PLELS 1000 (Polymer Laboratories, now Varian, Inc., Palo Alto, USA) and a Shimadzu SPD-10A VP UV/Vis detector operating at 220 and 254 nm. Preparative HPLC runs were performed on an Applied Biosystems workstation (Waltham, USA). Elution was performed using a gradient of 5% CH_3CN and 0.1% TFA in H_2O to 5% H_2O and 0.1% TFA in CH_3CN . ^1H NMR (400 MHz) and ^{13}C NMR (100 MHz) spectra were recorded on an Agilent 400-MR spectrometer (Santa Clara, USA). Heteronuclear single quantum coherence (HSQC) spectroscopy and total correlated spectroscopy (TOCSY) NMR (500 MHz) measurements were performed on a VARIAN INOVA-500 (Palo Alto, USA). Electrospray ionization mass spectrometry (ESI-MS) experiments were performed on a Shimadzu LCMS QP-8000. High resolution quadrupole-time-of-flight mass spectrometry (HRMS-QTOF) analysis was recorded using Bruker ESI-Q-TOF II (Billerica, USA). The proton numbering scheme of all compounds can be found in the Supporting Information and is used in the assignments of the signals in the NMR spectra here.

CTB_5 inhibition assay: A 96-well plate was coated with a solution of GM1 (100 μL , 2 $\mu\text{g mL}^{-1}$) in phosphate buffered saline (PBS). Unattached ganglioside was removed by washing with PBS twice,

and the remaining binding sites of the surface were blocked with BSA (1%), which was followed by washing with PBS three times. Samples of toxin–peroxidase conjugate (final concentration of 40 ng/ml CTB-HRP, Sigma) and inhibitor (final concentration of 10^{-6} – 10^{-12} M) in PBS with BSA (0.1%)/Tween-20 (0.05%) were incubated at rt for 2 h and were then transferred to the GM1-coated plate. After 30 min of incubation, the solution was removed and the wells were washed three times with PBS with BSA (0.1%)/Tween-20 (0.05%). To identify toxin binding to surface-bound GM1, the wells were treated with a freshly prepared solution of *o*-phenylenediamine/ H_2O_2 in citrate buffer (pH 4.5, 100 μL) for 15 min. After being quenched with H_2SO_4 (2.5 M, 50 μL), the absorbance in each well was measured at 490 nm. Inhibition data from three experiments were averaged and fitted in GraphPad Prism 5.0 (La Jolla, USA). (See Supporting Information for examples of the fitted data.)

Analytical ultracentrifugation experiments: Mixtures of CTB_5 with various amounts of inhibitors were prepared within 1 h before analysis was carried out. Samples (0.4 mL) were centrifuged in 12 mm pathlength 2-sector Al-centerpiece cells with sapphire windows in a An60Ti analytical rotor running in an Optima XL-I or Optima XL-A analytical ultracentrifuge (Beckman Instruments, Inc., Palo Alto, USA) at 60 krpm and at 25 °C. Changes in solute concentration were detected by 300 absorbance scans measured at 280 nm over a period of 5–6 h. Analysis and fitting of the data was performed using the software SedFit v.14.3.^[26] A continuous $c(s)$ distribution model was fitted to the data, taking every 2nd scan. The resolution was set at 200 over a sedimentation coefficient range of 0.0–15.0 S. Parameters were set for the partial specific volume as 0.73654 mL g^{-1} , the buffer density of 1.04910 g mL^{-1} , and the buffer viscosity at 0.00141 Pas, as calculated using SEDNTERP v.2.0 for 0.1 M PBS. The frictional coefficient, the baseline, and the raw data noise were floated in the fitting. The meniscus and bottom of the cell path were also floated after initial estimations from the raw data.

Compound 3: To a solution of tetraamine **1**^[5] (443 mg, 0.82 mmol) and spacer **2**^[21] (1.7 g, 3.90 mmol) in dry dimethylformamide (DMF, 15 mL), BOP (2.56 g, 5.79 mmol) and DIPEA (1.48 g, 11.48 mmol) were added. The mixture was stirred at rt overnight and then concentrated in vacuo. The residue was purified by silica gel chromatography to afford **3** (780 mg, 50%). ^1H and ^{13}C NMR were consistent with ref. [5] MS (ESI) m/z $[M+2H-2\times\text{Boc}]^{2+}$ calcd for $\text{C}_{105}\text{H}_{174}\text{N}_{14}\text{O}_{40}$: 1086.58, found 1086.75.

Compound 5: Compound **3** (780 mg, 0.33 mmol) was treated with TFA in CH_2Cl_2 (1:1, 20 mL) for 3 h at rt, after which the volatiles were removed under reduced pressure, and the residue was dried under high vacuum. Meanwhile, compound **4** was prepared following the literature procedure.^[22] The obtained amine TFA salt of **3** and the spacer **4** (670 mg, 2.30 mmol) were dissolved in anhydrous DMF (15 mL), then HATU (875 mg, 2.30 mmol) and DIPEA (892 mg, 6.90 mmol) were added. The mixture was stirred at rt overnight and then concentrated in vacuo. The residue was purified by silica gel chromatography to afford **5** (600 mg, 60%); ^1H NMR (400 MHz, CDCl_3): δ = 7.70, 7.58, 7.40, 6.81 (14H, 4 \times br t, J = 5 Hz, C(O)NH), 7.15 (2H, s, CH, aryl-2, aryl-6), 6.99 (4H, s, CH, 2 \times aryl-2', 2 \times aryl-6'), 6.70 (1H, s, CH, aryl-4), 6.54 (2H, s, CH, 2 \times aryl-4'), 4.17, 4.06 (12H, 2 \times br t, J = 5 Hz, $\text{OCH}_2\text{CH}_2\text{NH}$), 4.02, 3.99 (2 \times 8H, 2 \times s, $\text{OCH}_2\text{C(O)}$), 3.86 (3H, s, C(O)OCH₃), 3.82–3.75 (4H, m, $\text{OCH}_2\text{CH}_2\text{NH}$), 3.72–3.43 (120H, m, OCH_2 , $\text{OCH}_2\text{CH}_2\text{NH}$), 3.40–3.32 (16H, m, $\text{OCH}_2\text{CH}_2\text{N}_3$, $\text{CH}_2\text{NHC(O)}$), 3.32–3.24 (8H, m, $\text{CH}_2\text{NHC(O)}$), 2.42 (8H, t, J = 5 Hz, C(O)CH₂CH₂O), 1.82–1.66 ppm (16H, m, $\text{OCH}_2\text{CH}_2\text{CH}_2\text{NH}$); ^{13}C NMR (100 MHz, CDCl_3): δ = 171.16, 169.52, 168.85, 167.51 (C(O)NH), 166.68 (C(O)OCH₃), 159.84, 159.70 (C, aryl), 136.69 (C, aryl), 132.14

(C, aryl), 108.31 (CH, aryl-2, aryl-6), 106.76 (CH, aryl-4), 106.41 (CH, aryl-2', aryl-6'), 104.70 (CH, aryl-4'), 71.02 (OCH₂C(O)), 70.72–69.35 (OCH₂), 67.35 (OCH₂), 66.89, 66.62 (OCH₂CH₂NH), 52.40 (C(O)OCH₃), 50.74 (OCH₂CH₂N₃), 39.72, 38.46 (OCH₂CH₂NH), 37.22, 37.04 (CH₂NHC(O)), 36.81 (C(O)CH₂CH₂O), 29.38, 29.14 ppm (OCH₂CH₂CH₂NH); MS (ESI) *m/z* [*M*+3H]³⁺ calcd for C₁₃₄H₂₂₆N₂₆O₅₄: 1022.12, found 1022.40; HRMS (QTOF) *m/z* [*M*+3H]³⁺ calcd for C₁₃₄H₂₂₆N₂₆O₅₄: 1022.5257, found 1022.5348.

Compound 7: A solution of tetravalent **5** (7 mg, 2.28 μmol), **6** (14.8 mg, 13.4 μmol), sodium ascorbate (8.1 mg, 41.1 μmol), and CuSO₄·5H₂O (5.1 mg, 20.6 μmol) in DMF/H₂O (1:1, 2 mL) was prepared and heated under microwave irradiation at 80 °C for 20 min. After cooling down to rt, the copper salts were removed by a resin (Cuprisorb) and filtered off. The filtrate was then concentrated in vacuo, and the residue was purified by preparative HPLC and obtained by freeze-drying as an off-white powder (5 mg, 30%); ¹H NMR (500 MHz, D₂O): δ = 8.06, 7.96 (4H, 2×s, CH, triazole), 7.15 (2H, s, CH, aryl-2, aryl-6), 6.83 (5H, s, CH, 2×aryl-2', 2×aryl-6', aryl-4), 6.68 (2H, s, CH, 2×aryl-4'), 5.64, 5.15 (4H, 2×d, J_{1,2} = 8 Hz, J_{1,2} = 8 Hz, H_{Glc}-1), 4.79 (4H, H_{GalNAC}-1), 4.66–4.51 (24H, m, NCH₂C_{triazole}CH₂N_{triazole} H_{Gal}-1, H_{Gal}-1), 4.27–4.07 (12H, m, OCH₂CH₂NH), 4.10, 4.04 (2×8H, 2×s, OCH₂C(O)), 3.86 (3H, s, C(O)OCH₃), 3.77–3.65 (12H, m, OCH₂CH₂NH), 3.65–3.45 (112H, m, OCH₂), 3.41 (4H, t, J_{2,3} = J_{2,4} = 9 Hz, H_{Gal}-2), 3.31–3.17 (16H, m, CH₂NHC(O)), 2.69 (4H, dd, J_{3a,3b} = 13.5 Hz, J_{3a,4} = 4 Hz, H_{NeuAc}-3), 2.48 (8H, t, J = 6 Hz, C(O)CH₂CH₂O), 2.25 (12H, s, NC(O)CH₃), 2.04, 2.02 (2×12H, 2×s, NHC(O)CH₃), 1.96 (4H, t, J_{3b,3a} = J_{3b,4} = 11.5 Hz, H_{NeuAc}-3), 1.78–1.67 ppm (16H, m, OCH₂CH₂CH₂NH); ¹³C NMR (125 MHz, D₂O): δ = 175.54, 175.27, 174.64, 174.24, 171.71 (COOH, C(O)NH), 164.71 (C(O)OCH₃), 160.05 (C, aryl), 145.38 (C, triazole), 132.49 (C, aryl), 125.67, 125.42 (CH, triazole), 109.43 (CH, aryl-2, aryl-6), 106.94 (CH, aryl-2', aryl-6', aryl-4), 105.55 (CH, aryl-4'), 105.35 (C_{Gal}-1), 103.21 (C_{Gal}-1), 103.05 (C_{GalNAC}-1), 102.22 (C_{NeuAc}-2), 87.49, 82.91 (C_{Glc}-1), 80.79 (C_{GalNAC}-3), 78.65 (C_{Glc}-4), 77.41 (C_{Glc}-5), 77.30 (C_{Gal}-3), 75.50 (C_{Gal}-5), 75.11 (C_{Gal}-4), 75.07 (C_{GalNAC}-5), 75.06 (C_{Gal}-5), 73.62 (C_{NeuAc}-6), 73.07 (C_{Gal}-3), 72.54 (C_{NeuAc}-8), 71.28 (C_{Gal}-2), 70.60 (C_{Gal}-4), 70.54 (OCH₂C(O)), 70.50 (C_{NeuAc}-7, C_{Gal}-2), 70.49 (OCH₂C(O)), 70.12 (OCH₂), 70.02 (OCH₂), 69.99 (OCH₂), 69.25 (C_{GalNAC}-4), 69.02 (C_{NeuAc}-4), 68.96 (OCH₂), 68.49 (C_{Glc}-3), 67.49 (OCH₂CH₂NH), 67.38 (C_{Glc}-2), 67.25 (OCH₂CH₂NH), 63.48 (C_{NeuAc}-9), 61.55 (C_{GalNAC}-6, C_{Gal}-6), 61.05 (C_{Gal}-6), 60.66 (C_{Glc}-6), 53.39 (C(O)OCH₃), 52.15 (C_{NeuAc}-5), 51.86 (C_{GalNAC}-2), 50.71 (CH₂N_{triazole}), 40.36, 39.05 (OCH₂CH₂NH), 37.73 (C_{NeuAc}-3), 36.93 (CH₂NHC(O)), 36.75 (NCH₂C_{triazole}), 36.66 (C(O)CH₂CH₂O), 28.85 (OCH₂CH₂CH₂NH), 23.10 (C_{GalNAC}-NHC(O)CH₃), 22.61 (C_{NeuAc}-NHC(O)CH₃), 21.76 ppm (C_{Glc}-1-NC(O)CH₃); HRMS (QTOF) *m/z* [*M*-3H]³⁻ calcd for C₃₀₂H₄₈₆D₈N₃₈O₁₇₀: 2460.7688, found 2460.4179.

Compound 8: The obtained tetramer **5** (305 mg, 0.10 mmol) was treated with Tesser's base^[22] (dioxane/MeOH/4 N NaOH 30:9:1, 5 mL). The mixture was stirred at rt until the total disappearance of the starting material. After that, the reaction was quenched by adding 1 N KHSO₄, and the mixture was concentrated in vacuo. The residue was redissolved in CH₂Cl₂ (20 mL) and washed with 1 N KHSO₄ (10 mL), H₂O (10 mL), and brine (10 mL), dried on Na₂SO₄, and concentrated in vacuo. The resulting acid was used for the next step without further purification. To a solution of this acid and amine spacer **9** (O-(2-Aminoethyl)-O'-(2-azidoethyl)heptaethylene glycol, 70 mg, 0.16 mmol, Sigma–Aldrich) in dried DMF (10 mL), BOP (60 mg, 0.13 mmol) and DIPEA (40 mg, 0.31 mmol) were added. The mixture was stirred at rt overnight. Afterwards, the reaction was stopped and concentrated. The residue was suspended into CH₂Cl₂ (30 mL) and washed with 1 N KHSO₄ (15 mL), 1 N NaHCO₃ (15 mL), H₂O (15 mL), and brine (15 mL). The organic layer

was collected, dried on Na₂SO₄, and filtered. After concentration, the resulting material was purified by silica gel chromatography to afford **8** as a colorless oil (175 mg, 0.05 mmol, 51% over two steps); ¹H NMR (400 MHz, CDCl₃): δ = 7.76, 7.67, 7.58, 7.47, 6.87 (15H, 5×br t, J = 5 Hz, C(O)NH), 7.02 (2H, s, CH, aryl-2, aryl-6), 6.96 (4H, s, CH, 2×aryl-2', 2×aryl-6'), 6.63 (1H, s, CH, aryl-4), 6.52 (2H, s, CH, 2×aryl-4'), 4.17, 4.05 (12H, 2×b t, J = 5 Hz, OCH₂CH₂NH), 4.02, 3.98 (2×8H, 2×s, OCH₂C(O)), 3.80–3.72 (4H, m, OCH₂CH₂NH), 3.71–3.44 (152H, m, OCH₂, OCH₂CH₂NH), 3.40–3.31 (20H, m, OCH₂CH₂N₃, CH₂NHC(O)), 3.31–3.23 (8H, m, CH₂NHC(O)), 2.42 (8H, t, J = 5 Hz, C(O)CH₂CH₂O), 1.80–1.68 ppm (16H, m, OCH₂CH₂CH₂NH); ¹³C NMR (100 MHz, CDCl₃): δ = 171.69, 169.56, 168.91, 167.56, 167.29 (C(O)NH), 159.97, 159.70 (C, aryl), 136.82 (C, aryl), 136.69 (C, aryl), 106.48 (CH, aryl-2, aryl-6), 106.35 (CH, aryl-2', aryl-6'), 104.81 (CH, aryl-4), 104.72 (CH, aryl-4'), 71.02 (OCH₂C(O)), 70.73–69.36 (OCH₂), 67.38 (OCH₂), 66.75, 66.62 (OCH₂CH₂NH), 50.75 (OCH₂CH₂N₃), 40.01, 39.75, 38.49 (OCH₂CH₂NH), 37.22 (CH₂NHC(O)), 36.93 (C(O)CH₂CH₂O), 29.39, 29.18 ppm (OCH₂CH₂CH₂NH); MS (ESI) *m/z* [*M*+3H]³⁺ calcd for C₁₅₁H₂₆₀N₃₀O₆₁: 1157.61, found 1157.65, [*M*+2H]²⁺ calcd for 1736.91, found 1736.65; HRMS (QTOF) *m/z* [*M*+3H]³⁺ calcd for C₁₅₁H₂₆₀N₃₀O₆₁: 1157.6055, found 1157.9647.

Compound 10: A solution of pentavalent scaffold **8** (8.4 mg, 2.42 μmol), **6** (16 mg, 14.55 μmol), sodium ascorbate (6.92 mg, 35 μmol), and CuSO₄·5H₂O (4.35 mg, 17.4 μmol) in DMF/H₂O (1:1, 2 mL) was prepared and heated under microwave irradiation at 80 °C for 20 min. After cooling down to rt, the copper salts were removed by a resin (Cuprisorb) and filtered off. The filtrate was then concentrated in vacuo, and the residue was purified by preparative HPLC and obtained by freeze-drying as an off-white powder (8.7 mg, 41%); ¹H NMR (500 MHz, D₂O): δ = 8.07, 7.96 (5H, 2×s, CH, triazole), 7.02 (2H, s, CH, aryl-2, aryl-6), 6.85, 6.80 (5H, 2×s, CH, 2×aryl-2', 2×aryl-6', aryl-4), 6.70 (2H, s, CH, 2×aryl-4'), 5.64, 5.15 (5H, 2×d, J_{1,2} = 8.5 Hz, J_{1,2} = 8.5 Hz, H_{Glc}-1), 4.78 (5H, H_{GalNAC}-1), 4.67–4.52 (30H, m, NCH₂C_{triazole}CH₂N_{triazole} H_{Gal}-1, H_{Gal}-1), 4.27–4.09 (12H, m, OCH₂CH₂NH), 4.11, 4.05 (2×8H, 2×s, OCH₂C(O)), 3.76–3.65 (12H, m, OCH₂CH₂NH), 3.68–3.45 (146H, m, OCH₂, CH₂NHC(O)), 3.40 (5H, t, J_{2,3} = J_{3,4} = 9 Hz, H_{Gal}-2), 3.29–3.19 (16H, m, CH₂NHC(O)), 2.69 (5H, dd, J_{3a,3b} = 13 Hz, J_{3a,4} = 4 Hz, H_{NeuAc}-3), 2.49 (8H, t, J = 6 Hz, C(O)CH₂CH₂O), 2.26 (15H, s, NC(O)CH₃), 2.04, 2.02 (2×15H, 2×s, NHC(O)CH₃), 1.96 (5H, t, J_{3b,3a} = J_{3b,4} = 11 Hz, H_{NeuAc}-3), 1.80–1.69 ppm (16H, m, OCH₂CH₂CH₂NH); ¹³C NMR (125 MHz, D₂O): δ = 175.54, 175.28, 174.29, 174.14, 172.33, 171.75 (COOH, C(O)NH), 160.07 (C, aryl), 145.47 (C, triazole), 136.36 (C, aryl), 125.41, 125.39 (CH, triazole), 107.40 (CH, aryl-2, aryl-6), 106.89 (CH, aryl-2', aryl-6'), 106.01 (CH, aryl-4), 105.51 (CH, aryl-4'), 105.28 (C_{Gal}-1), 103.16 (C_{Gal}-1), 103.01 (C_{GalNAC}-1), 101.76 (C_{NeuAc}-2), 87.38, 82.87 (C_{Glc}-1), 80.77 (C_{GalNAC}-3), 78.59 (C_{Glc}-4), 77.38 (C_{Gal}-3), 77.32 (C_{Glc}-5), 75.45 (C_{Gal}-5), 75.03 (C_{GalNAC}-5), 74.98 (C_{Gal}-4), 74.73 (C_{Gal}-5), 73.64 (C_{NeuAc}-6), 73.04 (C_{Gal}-3), 72.56 (C_{NeuAc}-8), 71.16 (C_{Gal}-2), 70.59 (C_{NeuAc}-7, C_{Gal}-2), 70.44 (OCH₂C(O)), 70.37 (OCH₂C(O)), 70.16 (C_{Gal}-4), 70.10 (OCH₂), 70.09 (OCH₂), 70.03 (OCH₂), 69.14 (C_{GalNAC}-4), 68.97 (C_{NeuAc}-4), 68.94 (OCH₂), 68.43 (C_{Glc}-3), 67.41 (OCH₂CH₂NH), 67.32 (C_{Glc}-2), 67.26 (OCH₂CH₂NH), 63.41 (C_{NeuAc}-9), 61.49 (C_{GalNAC}-6, C_{Gal}-6), 60.88 (C_{Gal}-6), 60.61 (C_{Glc}-6), 52.10 (C_{NeuAc}-5), 51.76 (C_{GalNAC}-2), 50.60 (CH₂N_{triazole}), 40.19, 40.17, 39.01 (OCH₂CH₂NH), 37.61 (C_{NeuAc}-3), 36.83 (CH₂NHC(O)), 36.70 (NCH₂C_{triazole}), 36.59 (C(O)CH₂CH₂O), 28.78 (OCH₂CH₂CH₂NH), 23.08 (C_{GalNAC}-NHC(O)CH₃), 22.58 (C_{NeuAc}-NHC(O)CH₃), 21.68 ppm (C_{Glc}-1-NC(O)CH₃); HRMS (QTOF) *m/z* [*M*+5H+NH₄]⁶⁺ calcd for C₃₆₁H₅₉₁D₄N₄₅O₂₀₆: 1481.1261, found 1481.4361.

Acknowledgements

This research is supported by the Dutch Technology Foundation (STW), Applied Science Division of the Netherlands Organization for Scientific Research (NWO), Technology Program of the Ministry of Economic Affairs, and by European Cooperation in Science and Technology (COST) Action CM1102 MultiGlycoNano.

Keywords: cholera toxin · CuAAC click conjugation · glycodendrimers · GM1 oligosaccharide · multivalency

- [1] E. A. Merritt, W. G. J. Hol, *Curr. Opin. Struct. Biol.* **1995**, *5*, 165–171.
- [2] L. De Haan, T. R. Hirst, *Mol. Membr. Biol.* **2004**, *21*, 77–92.
- [3] C. Fasting, C. A. Schalley, M. Weber, O. Seitz, S. Hecht, B. Kokschi, J. Dernecke, C. Graf, E.-W.-W. Knapp, R. Haag, *Angew. Chem. Int. Ed.* **2012**, *51*, 10472–10498; *Angew. Chem.* **2012**, *124*, 10622–10650.
- [4] R. J. Pieters, *Org. Biomol. Chem.* **2009**, *7*, 2013–2025.
- [5] D. Arosio, I. Vrasidas, P. Valentini, R. M. J. Liskamp, R. J. Pieters, A. Bernardi, *Org. Biomol. Chem.* **2004**, *2*, 2113–2124.
- [6] H. M. Branderhorst, R. M. J. Liskamp, G. M. Visser, R. J. Pieters, *Chem. Commun.* **2007**, 5043–5045.
- [7] H.-A. Tran, P. I. Kitov, E. Paszkiewicz, J. M. Sadowska, D. R. Bundle, *Org. Biomol. Chem.* **2011**, *9*, 3658–71.
- [8] S.-J. Richards, M. W. Jones, M. Hunaban, D. M. Haddleton, M. I. Gibson, *Angew. Chem. Int. Ed.* **2012**, *51*, 7812–6; *Angew. Chem.* **2012**, *124*, 7932–7936.
- [9] S. Liu, K. L. Kiick, *Macromolecules* **2008**, *41*, 764–772.
- [10] E. K. Fan, Z. S. Zhang, W. E. Minke, Z. Hou, C. L. M. J. Verlinde, W. G. J. Hol, V. Uni, *J. Am. Chem. Soc.* **2000**, *122*, 2663–2664.
- [11] J. Garcia-Hartjes, S. Bernardi, C. A. G. M. Weijers, T. Wennekes, M. Gilbert, F. Sansone, A. Casnati, H. Zuilhof, *Org. Biomol. Chem.* **2013**, *11*, 4340–9.
- [12] M. Mattarella, J. Garcia-Hartjes, T. Wennekes, H. Zuilhof, J. S. Siegel, *Org. Biomol. Chem.* **2013**, *11*, 4333–9.
- [13] T. R. Branson, W. B. Turnbull, *Chem. Soc. Rev.* **2013**, *42*, 4613–22.
- [14] V. Wittmann, R. J. Pieters, *Chem. Soc. Rev.* **2013**, *42*, 4492–4503.
- [15] Z. Zhang, E. a. Merritt, M. Ahn, C. Roach, Z. Hou, C. L. M. J. Verlinde, W. G. J. Hol, E. Fan, *J. Am. Chem. Soc.* **2002**, *124*, 12991–12998.
- [16] S. Cecioni, A. Imbert, S. Vidal, *Chem. Rev.* **2015**, *115*, 525–561.
- [17] A. V. Pukin, H. M. Branderhorst, C. Sisu, C. C. A. G. M. Weijers, M. Gilbert, R. M. J. Liskamp, G. M. Visser, H. Zuilhof, R. J. Pieters, *ChemBioChem* **2007**, *8*, 1500–1503.
- [18] C. Sisu, A. J. Baron, H. M. Branderhorst, S. D. Connel, C. C. A. G. M. Weijers, R. de Vries, E. D. Hayes, A. V. Pukin, M. Gilbert, R. J. Pieters, H. Zuilhof, G. M. Visser, W. B. Turnbull, *ChemBioChem* **2009**, *10*, 329–337.
- [19] T. R. Branson, T. E. McAllister, J. Garcia-Hartjes, M. A. Fascione, J. F. Ross, S. L. Warriner, T. Wennekes, H. Zuilhof, W. B. Turnbull, *Angew. Chem. Int. Ed.* **2014**, *53*, 8323–7; *Angew. Chem.* **2014**, *126*, 8463–8467.
- [20] P. I. Kitov, J. M. Sadowska, G. Mulvey, G. D. Armstrong, H. Ling, N. S. Pannu, R. J. Read, D. R. Bundle, *Nature* **2000**, *403*, 669–672.
- [21] R. Autar, A. S. Khan, M. Schad, J. Hacker, R. M. J. Liskamp, R. J. Pieters, *ChemBioChem* **2003**, *4*, 1317–1325.
- [22] H. Herzner, H. Kunz, *Carbohydr. Res.* **2007**, *342*, 541–557.
- [23] P. Schuck, M. A. Perugini, N. R. Gonzales, G. J. Hewlett, D. Schubert, *Biophys. J.* **2002**, *82*, 1096–1111.
- [24] J. Lebowitz, M. S. Lewis, P. Schuck, *Protein Sci.* **2009**, *11*, 2067–2079.
- [25] P. I. Kitov, D. R. Bundle, *J. Am. Chem. Soc.* **2003**, *125*, 16271–16284.
- [26] P. Schuck, *Biophys. J.* **2000**, *78*, 1606–1619.

Received: January 6, 2015

Published online on March 21, 2015